Hindawi
Advances in Civil Engineering
Volume 2021, Article ID 6622418, 17 pages
https://doi.org/10.1155/2021/6622418

Research Article

Experimental Study of the Failure Mechanism of the Anchorage Interface under Different Surrounding Rock Strengths and Ambient Temperatures

Xiaohu Liu,[1] **Zhishu Yao**,[1] **Weipei Xue**,[1,2] **Xuesong Wang**,[1] **and Xianwen Huang**[1]

[1]*School of Civil Engineering and Architecture, Anhui University of Science and Technology, Huainan 232001, China*
[2]*Post-Doctoral Research Station of Safety Science and Engineering, Anhui University of Science and Technology, Huainan 232001, China*

Correspondence should be addressed to Zhishu Yao; zsyao@aust.edu.cn

Received 24 December 2020; Revised 4 March 2021; Accepted 20 April 2021; Published 3 May 2021

Academic Editor: Yingchun Li

In order to study the anchoring instability mechanism of surrounding rock in deep roadway, the failure mechanism of the bolt-anchoring agent interface was studied by simulating different strength rock mass and ground temperature environment, using C20, C40, and C60 strength concrete and steel pipe to simulate different surrounding rock strength environments. Indoor pull-out tests were carried out to study the pull-out load displacement relationship, ultimate pull-out force, residual anchoring force, the distribution law of axial stress and tangential stress along the bar, and the energy consumption value of drawing failure at 20, 50, and 70°C. The test results show that, with the decrease of surrounding rock strength or the increase of ambient temperature, the pull-out force, residual anchoring force, and energy consumption value of anchorage interface gradually decrease; under different axial forces, the axial force distribution of the rod body decreases exponentially from the anchoring end to the opposite end; and the shear stress transfers to the deep part of the anchor body with the increase of the load. According to the failure phenomenon of the specimen, the failure modes of the bolt bolt-anchorage agent interface can be divided into shear slip mode and shear expansion slip mode. The shear expansion slip formula of anchorage interface is derived. Using high-strength and temperature-resistant resin anchoring agent for comparative test, the rationality of the mechanism analysis is proved, which provides more clear guidance for the construction of anchor support.

1. Introduction

With many coal mines entering deep coal seam mining, supporting problems such as high ground stress, high ground temperature, broken surrounding rock, or weak stratum appear in roadway construction, with large deformation and strong rheology of surrounding rock mass [1–3]. Under complex geological conditions, the surrounding rock support of deep roadway is difficult, and the bolt loss rate of support bolt increases gradually. The supporting bolt interacts with the surrounding rock to form a whole with the surrounding rock and bear the load generated by the deformation of surrounding rock [4–6]. Generally, the anchoring support system is composed of surrounding rock, anchoring agent, and bolt. The failure mode of anchorage interface is the most common, but the failure mechanism of anchorage interface is still unclear [7–10]. In order to ensure the efficient and safe mining of deep resources, it is necessary to further study the failure law of anchor under different surrounding rock strength and ambient temperature.

Many scholars have studied the failure of anchorages under different environmental conditions. In high-temperature and room temperature environments, Zhang Sheng studied the influence of water and temperature on the anchor hold of a resin anchoring bolt in the laboratory under two conditions, namely, water moving in the borehole and water accumulating in the borehole. The conclusion reached was that the impact of water on the borehole wall and the increase of the borehole wall temperature will reduce the anchoring ability of the general resin [11]. Huet al. studied

the influence of temperature on the anchoring performance of a resin anchor by combining a laboratory test and numerical simulation. The results showed that the anchoring force of the anchorage body was the largest at 25°C, and the anchoring force clearly decreased with the increase of simulated drilling temperature [12]. Based on the thick wall theory, Zhao and other researchers studied the relationship between anchor rib spacing and anchorage performance under different country rock conditions. Under arbitrary country rock conditions, increasing rib spacing can improve the anchoring performance [13]. Li Fuhai et al. researched the influence of temperature on the bond behavior of the anchoring interface. Through a test of a fully grouted bolt in an indoor simulation of high temperature, it was concluded that with the increase of the ambient temperature of the anchor body the maximum shear stress of the bolt section decreases, and the shear stress distribution along the bolt section is more uniform [14]. The tests of Li were carried out to study the pull-out failure strength of anchors under different temperatures and roughness conditions. The results showed that temperature has little influence on the pull-out failure with cement grout as a binder. With the increase of country rock roughness, the pull-out strength of the anchor body increases, and the bolt support effect is enhanced [15]. Su et al. studied the pyrolysis characteristics and pore structure evolution of resin anchoring materials at high temperature using micro CT scanning and three-dimensional image reconstruction technology. It was concluded that high temperature had a significant impact on the internal structure and density of the materials. At high temperature, the mechanical properties of the material decreased significantly, the compressive strength decreased by 95%, and the pull-out resistance decreased by 68.3% [16]. Li carried out research on thermomechanical coupling of an anchor solid in a deep mine roadway, tested the mechanical properties of an anchoring agent at different temperatures, and carried out a bolt pull-out test to study the influence of a high ground temperature environment on the anchoring mechanism [17]. Pothisiri used a mechanical model of bonding between steel rebar and concrete at elevated temperatures based on the smear crack theory and a thick-wall cylinder in its partially cracked elastic stage. The results showed that the compressive strength of concrete, the thickness of the protective layer, and temperature change will lead to the degradation of bond strength [18]. Based on the research results of the above scholars, it has been shown that temperature, presence of water, and strength and roughness of country rock all affect the pull-out strength of anchors. However, the failure mechanism remains unclear. In particular, the failure mechanism of the anchoring interface for a bolt support system with a resin anchoring agent as the binder has been little studied. It is of great significance to determine the failure mechanism of bolts by studying the failure law of anchorage interfaces in different environments.

This study used a bolt supporting system with a resin anchoring agent as the bonding material and examined the failure law of the resin-anchor interface under different temperature and country rock strength environments. This study conducted indoor pull-out tests using a self-made bolt drawing mold; C20, C40, and C60 strength concrete columns; and a steel pipe to simulate different country rock strength and temperature environments. Analyzed parameters were the pull-out load-displacement relationship, interface axial stress, shear stress distribution rule, and pull-out failure energy consumption value of the anchorage interface under different environments. The influence of temperature and the country rock strength on the failure of the anchor solid interface was revealed. Finally, using high-strength and temperature resistant resin anchoring agent for comparative test, the rationality of the mechanism analysis is proved, and the method of optimizing the strength of anchor body is obtained to increase the pull-out load of anchorage interface, which provides more clear guidance for the construction of anchor support.

2. Test Materials and Preparation

2.1. Anchor Material and Preparation of Force Measuring Bolt. MSGLW-500, a left lateral screw-thread steel bolt without longitudinal reinforcement, was selected for the test. Its structure and mechanical properties are shown in Table 1 [19]. The bolt was cut into 500 mm long segments, and a monitoring strain gauge was installed to construct a pull-out force measuring bolt. The specimen construction and strain gauge arrangement are shown in Figure 1.

The anchor rod in Figure 1(a) was divided into three sections, namely, the anchoring section (300 mm), the exposed section (160 mm), and the mixing section (40 mm). The anchoring section was bonded with the country rock with resin anchoring agent; the exposed section was clamped by the pull-out testing machine; and the mixing section was a smooth round rod with a diameter of 12 mm and was used by an electric drill to secure the anchor bolt into the country rock. Cut off the mixing section after the mixing anchor. Two side symmetrical milling grooves (width × depth = 6 × 3 mm) were used to arrange strain gauges and wires in the anchorage and exposed sections. The cross section is shown in Figure 1(b). Bx120-3aa strain gauges were used. The grid dimensions (length × width) were 3 × 2 mm and the resistance was 120 ± 0.1 Ω. The specific arrangement is shown in the diagram in Figure 1(a). Seven strain gauges were arranged in total, and the strain gauges arranged from the beginning to the end of the anchor bolt were numbered as 1~7#; 1# was located at the exposed section, 20 mm from the beginning of the anchoring section, and the spacing between 1 and 7# was 50 mm, with a total monitoring range of 300 mm. Before arranging the strain gauge, the groove was ground with sandpaper and cleaned with acetone; the strain gauge was then pasted into the groove with 520 glue and the wire was welded. When the glue was dry, the gap in the groove was filled with epoxy resin glue; the anchor is shown in Figure 1(a).

2.2. Anchoring Agent. The medium speed full-length anchoring agent was selected for the test. The anchoring agent has high strength and short gelation time, which meet the

Table 1: Structure and mechanical parameters of the MSGLW-500 bolt.

Diameter (mm)	Rib height (mm)	Rib spacing (mm)	Cross-sectional area (mm^2)	Modulus of elasticity (GPa)	Yield strength (kN)	Breaking strength (kN)
22	1	**12**	379.94	200	190	239

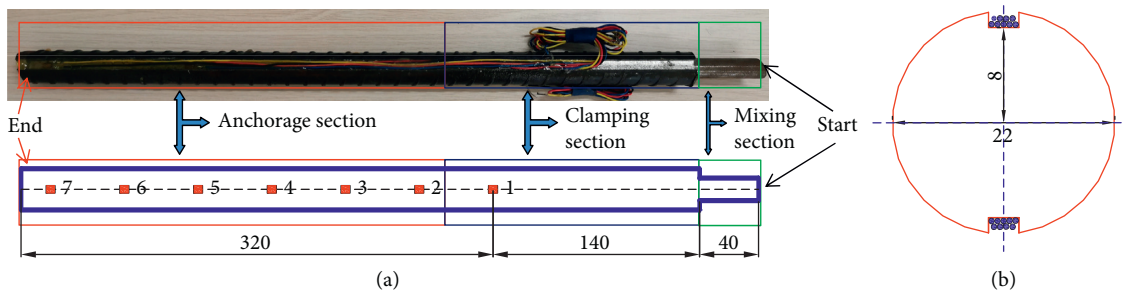

Figure 1: Strain gauge layout of force measuring bolt (unit: mm).

needs of rapid support in a deep mine roadway. The curing dosage of the anchoring agent is 4% of the mass of the resin mortar, the curing time is 180 s, the strength of the anchoring agent is 65 MPa, the elastic modulus is 10.5 GPa, and Poisson's ratio is 0.26. In addition, the compressive strength of the anchoring agent at different temperatures is shown in Table 2 [20, 21].

2.3. Country Rock Material and Specimen Preparation. Hard rock, medium strong rock, and weak rock exist in the country rock of roadway bolt supports. To simulate the mechanical properties of bolts under different country rock strength conditions, seamless steel pipes and concrete with different strengths were designed to simulate different country rock strengths. Steel pipe is used to simulate hard rock formation, C60 and C40 strength concrete were prepared to simulate medium strong country rock, and C20 strength concrete was used to simulate soft country rock. Considering the three-diameter ratio and the influence range of the anchor rod, the outer diameter of the steel pipe was 42 mm, the wall thickness was 5 mm, the length of the steel pipe was 300 mm, the elastic modulus was 206 GPa, and Poisson's ratio was 0.3. The outer diameter of concrete country rock was 150 mm, the inner diameter was 32 mm, and the height was 300 mm. According to the relevant literature, a reasonable mix proportion of concrete was selected [22, 23]. The mix numbers of C60, C40, and C20 strength concrete are shown in Table 3.

In addition, the concrete country rock sample was poured using a concrete block mold with inner diameter × height = 150 × 300 mm. Before pouring, a PVC pipe with length of 450 mm and outer diameter of 32 mm was vertically placed in the center of the mold. The mixture was introduced into the mold and vibrated evenly on the vibration table, and the end face was smoothed with a flat shovel. After 2~3 hours, the PVC pipe was extracted, and the concrete column was removed from the mold and subjected to standard curing after 24 hours. It was cured in the protective box for 28 days. The test results showed that the compressive strength of C60, C40, and C20 concrete samples was 67.2, 48.3, and 29.1 MPa, respectively, and thus met the study requirements.

2.4. Preparation of the Drawing Test Specimen. The steel pipe end and the two ends of the cured concrete country rock sample were polished with a grinder. The amount of anchoring agent required for each specimen was calculated and weighed and put into the pre-reserved anchor hole. Then, the electric drill was used to clamp the anchor rod mixing section to quickly mix and push it into the designed anchor length. After anchoring, the specimens were cured at room temperature for 24 hours; finished specimens are shown in Figures 2 and 3.

3. Test Device and Scheme

3.1. Construction of Bolt Drawing Test Mold. To facilitate the pull-out test of the anchor body, alloy steel was selected as the material of the mold after repeated attempts. The test diagram and structural design are shown in Figure 4.

It can be seen from Figure 4 that the mold was composed mainly of upper and lower limit plates and connecting bolts. The lower limit plate center was vertically welded to a steel bar with a length of 150 mm and diameter of 22 mm, which was used for clamping the drawing testing machine. The upper and lower limit plates were 30 mm thick. The two plates were connected by six screws. The diameter of each screw was 16 mm and the length was 400 mm. To test the pull-out failure strength of the bolt-anchorage agent interface, a hole with a diameter of 22.5 mm was reserved in the center of the upper limit plate to guide the bolt, as shown in Figure 4(c). The force mode of the pull-out specimen is shown in Figure 4(b).

3.2. Specimen Heating and Temperature Control Devices. To accurately simulate the ambient temperature, a heating ring was used to heat the specimen. The heating ring is shown in Figure 5. A stainless steel heating ring with an

Table 2: Compressive strength of the anchoring agent in different temperature environments.

Type	20°C	50°C	80°C	110°C
General	65 MPa	39.4 MPa	27.5 MPa	15 MPa

Table 3: Concrete mix proportions.

Strength grade	Cement (kg)	Sand (kg)	Stone (kg)	Water (kg)	Sand rate (%)	Type sand parameters of water reducing agent (kg)
C20	350 (P.O 32.5)	680.8	1159.2 (limestone)	210	37	—
C40	400 (P.O 42.5)	705.22	1200.8 (limestone)	144	37	NF(5.6)
C60	420 (P.O 42.5)	648.1	1103.4 (basalt)	148.5	37	NF-F(130)

Figure 2: Steel tube country rock specimens.

Figure 3: Concrete country rock specimens.

inner diameter of 42 mm and height of 80 mm was used for the steel pipe simulation of country rock, and a ceramic heating ring with an inner diameter of 150 mm and height of 100 mm was used for the concrete simulation of country rock. In addition, a xmtd-2001 digital display temperature controller was used, which was composed of 220 V AC contactor, screw type sensor, and K-type temperature sensor. For the specimen using the steel pipe to simulate the country rock, the outer wall of the steel pipe was welded with an M6 nut to connect a screw-type sensor; for the specimen using concrete to simulate country rock, a hole with a diameter of 8 mm and depth of 60 mm was drilled on the central side wall of the concrete column to insert a K-type temperature sensor. Ceramic heating ring and stainless-steel heating ring are directly sheathed in the concrete surrounding rock and steel pipe outer wall, respectively, and both are placed in the drawing die together. The power line of the heating ring is penetrated from the mold ring to the column. Before the pull-out test, the test piece was heated, the required temperature in the temperature controller was set, and the temperature sensor was inserted into the test piece. When the temperature of the heating sample exceeded the set temperature, the temperature meter controlling the AC contactor cut off the power supply. Thus, after several iterations of repeated heating to ensure the temperature in the anchorage specimen was uniform and constant, the pull-out test was carried out.

3.3. Drawing Test Equipment and Test Scheme. A Waw-1000c microcomputer-controlled electrohydraulic servo universal testing machine was used to pull out the bolt. The maximum test force of the testing machine was 1000 kN. Hydraulic clamping was used in the test, with a clamping diameter of Φ 12~Φ 60 mm and net spacing of the column of 650 mm. The axial stress of the bolt was monitored by a YE2539 dynamic strain gauge.

The prepared drawing specimen was installed in the drawing die and placed on the universal testing machine clamp. During the test, displacement of 2 mm/min was used to control the loading. The test system is shown in Figure 6. The failure process of pull-out specimens with different country rock strength (C20, C40, C60, steel pipe) was simulated at different ambient temperatures (20, 50, 70°C).

4. Analysis and Interpretation of Test Results

In the pull-out test, the anchor was subjected to increasing axial force until the anchorage failed. Because the bolt hole on the hanging wall of the drawing die was essentially consistent with the outer diameter of the bolt, the pull-out failure was limited to the interface between the bolt and the anchoring agent. Monitoring and collating the data, the following results were obtained.

4.1. Pull-Out Load Displacement. According to the test scheme, the pull-out test was carried out; the load displacement relationship of each pull-out specimen is shown in Figure 7.

It can be seen from Figure 7 that with the increase of the pull-out displacement the pull-out force of all of the bolts increases rapidly at first and then decreases; with the increase of the country rock strength of the bolt specimen, the

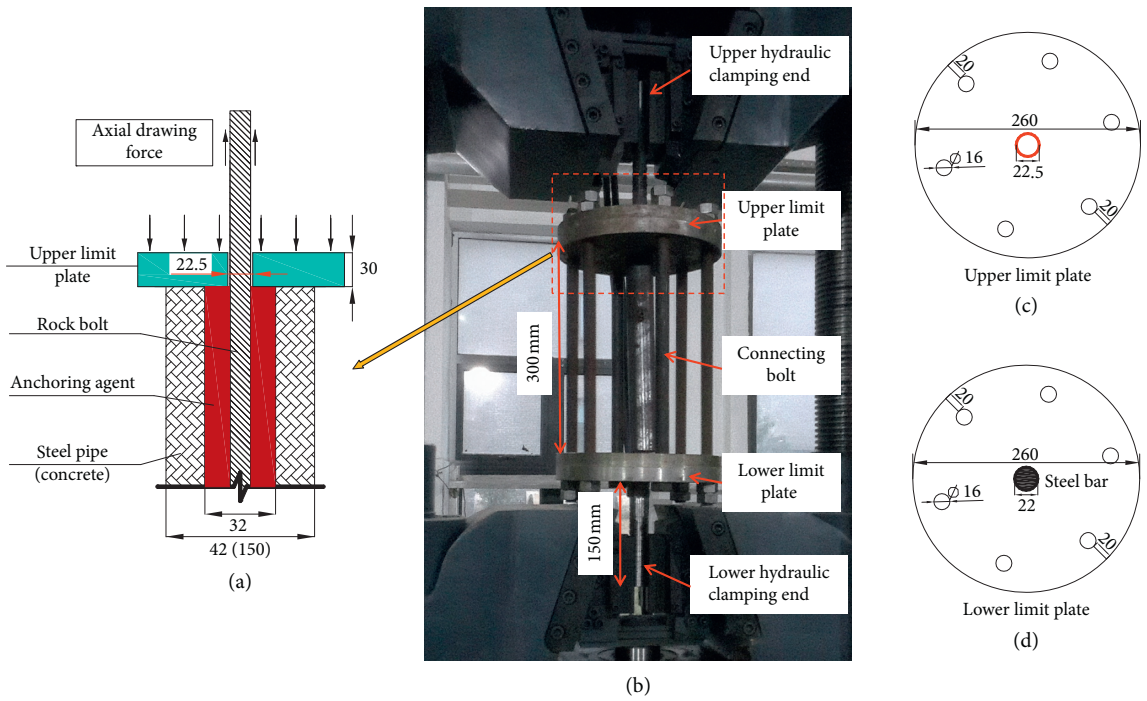

FIGURE 4: Structure of pull-out test tool (unit: mm).

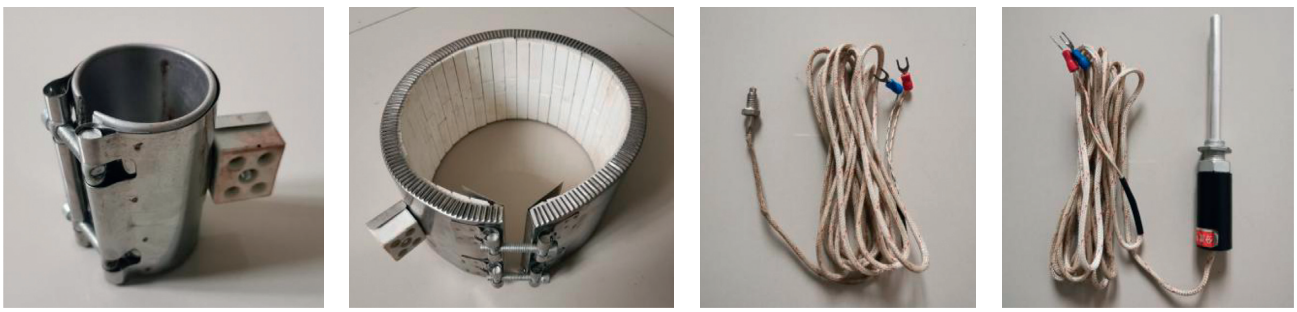

FIGURE 5: Heating ring and temperature sensor of drawing specimen: (a) a stainless-steel heating ring; (b) a ceramic heating ring; (c) screw type sensor; (d) K-type temperature sensor.

maximum anchoring force increases gradually. The peak value of the pull-out force of the concrete country rock anchor is in the range of 7.5~17.5 mm. The load-displacement development process can be divided into four stages: ① elastic stage(A-B): the pull-out load and displacement of the anchor bolt increase linearly, the pulling load of the anchor solid increases rapidly, and the displacement of the anchor bolt is mainly elastic deformation. ② Plastic deformation stage (B-C): the anchorage interface in the anchor body enters the plastic deformation stage under the action of shear force. In this stage, the displacement of the anchor rod increases rapidly, and the pull-out load of the bolt continues to increase slightly. This stage is clear in the drawing of the st-20 °C specimens but was not clearly evident for the remainder of the specimens. ③ Failure stage of anchor loss (C-D): after reaching the strength limit of the anchor body, the continuous increase of the pull-out load leads to the debonding failure of the anchorage interface, resulting in the dramatic decrease of the anchor load. ④ Residual strength stage (D-E): when the whole anchor body debonds, the axial slip of the anchorage interface produces the interface friction, the displacement of the anchor increases rapidly, and the friction resistance decreases slowly.

In Figure 7(a), the yield stage of the steel pipe simulation of the country rock anchor solid in the normal temperature environment lasts for a long time. When the anchor body is damaged, shear failure occurs at the interface. The country rock of the steel pipe provides greater holding force for the anchorage body. At normal temperature, the strength of the adhesive anchorage agent is high, and the interface has strong shear resistance. With the increase of temperature, the shear strength of the anchorage agent decreases, the anchorage interface fails more rapidly, and the anchorage length of the specimen is shorter; therefore, the yield stage of

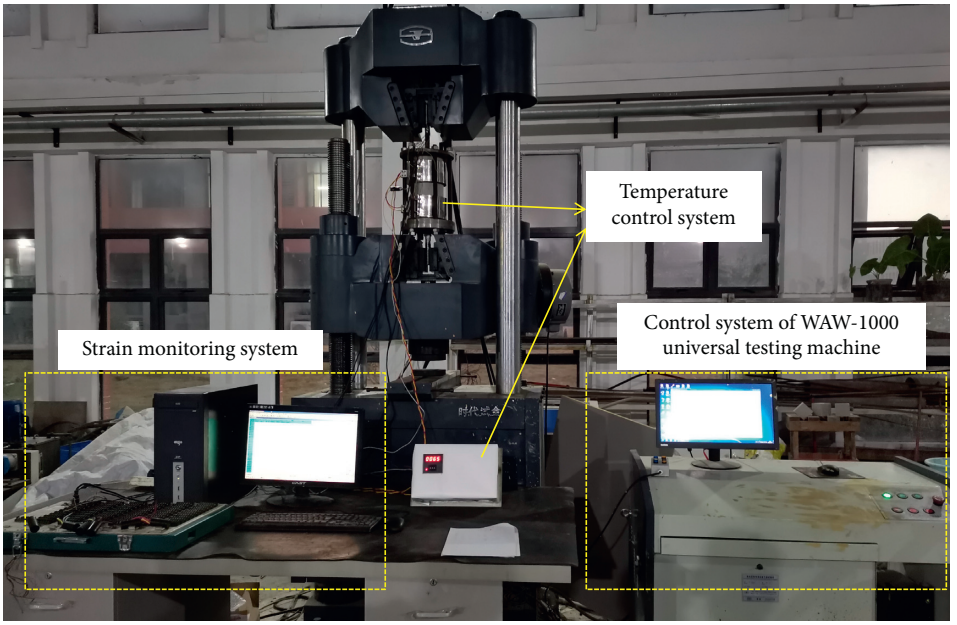

Figure 6: Pull-out test system of bolt.

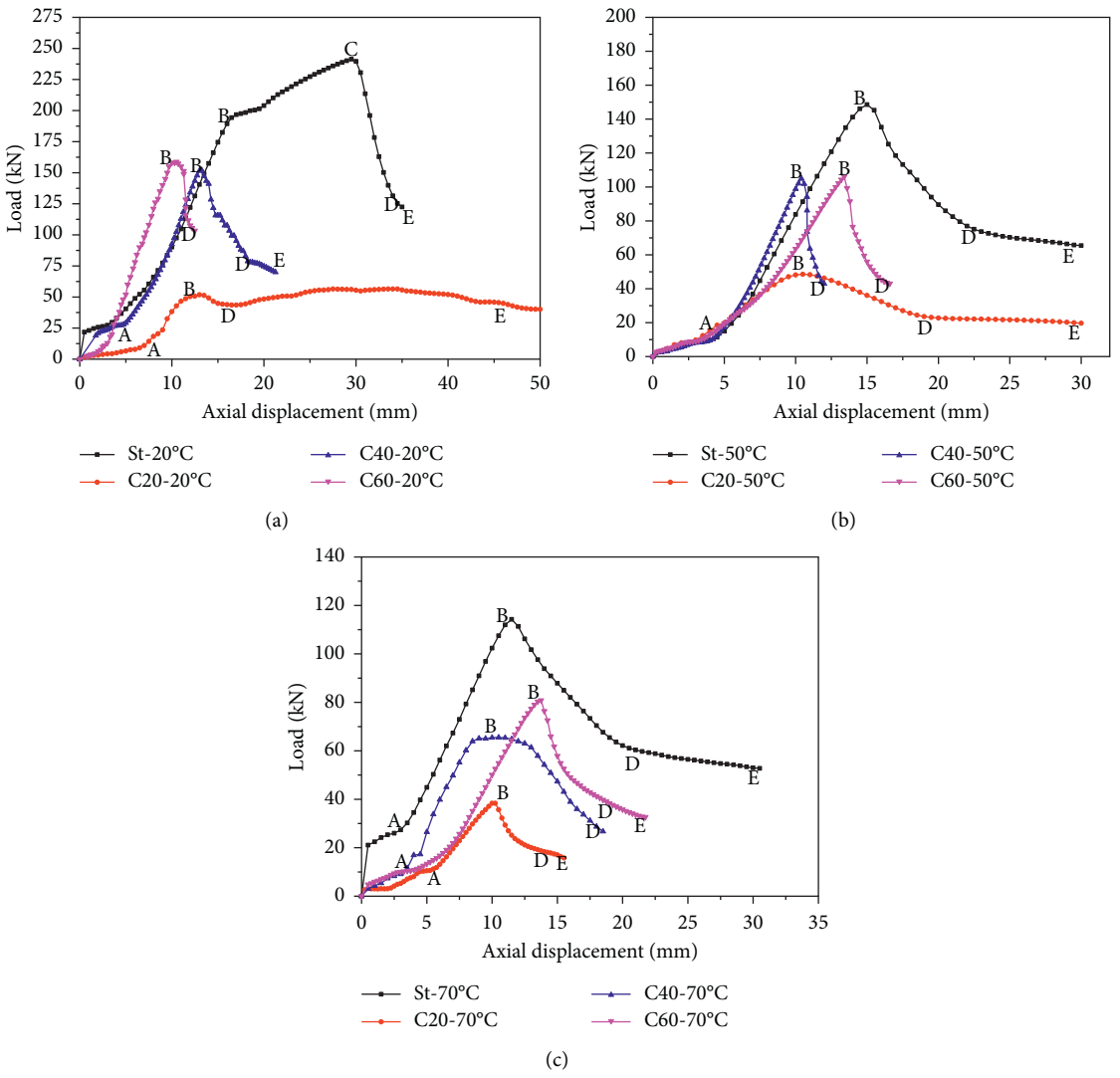

Figure 7: Relationship between drawing force and displacement. (a) Pull-out specimens in 20°C. (b) Pull-out specimens in 50°C. (c) Pull-out specimens in 70°C.

the anchor solid is not obvious. In addition, as shown in Figure 7(b) and 7(c), the yield stage is also missing in the process of the concrete simulation of the country rock anchor pull-out. The reason is that the anchor loss is accompanied by radial cracking of the concrete country rock. After the country rock is damaged, the anchor body enters the stage of anchor loss failure. The lower the strength of country rock, the smaller the peak value of the pull-out force.

4.2. Ultimate Pull-Out Strength and Residual Anchoring Force. The ultimate pull-out force and residual drawing anchoring force of the anchor solid interface under different country rock strengths and temperature environments are shown in Figures 8 and 9, respectively.

It can be seen from Figure 8 that the ultimate tensile strength of the anchorage interface decreased by 38.8% and 52.9%, respectively, at 50 and 70°C relative to 20°C; the ultimate tensile strength of C20, C40, and C60 country rock, respectively, decreased by 14.5%, 29.6%, and 25.3% at 50°C and 31.6%, 56.9%, and 51.5% at 70°C relative to 20°C. It can be seen from the above results that with the increase of country rock strength the change range of the ultimate pull-out strength of the anchorage interface increased with temperature. However, when the strength of country rock was C40 and C60, the difference of the ultimate pull-out force of the anchorage interface in the same temperature environment was small, and the change range of the ultimate strength at different temperatures was similar.

When the anchor body is subjected to axial stress, both axial and radial shear forces along the radial direction of the country rock are produced at the interface between the anchor and the anchoring agent. The shear force acts on the anchoring agent and the country rock through the anchoring interface. If the strength of the country rock is substantially less than that of the anchorage agent itself, the tensile shear failure of the country rock will occur due to the shear force. The country rock cannot provide enough binding force, and the anchoring force of the anchoring interface decreases rapidly; at this time, the ultimate pull-out force of the anchorage interface is limited by the strength of the country rock. when the strength of resin anchoring agent is approximately equal to the strength of surrounding rock, with the increase of axial pull-out force on the anchor body, radial shear dilatation failure will occur at the interface between anchor and anchoring agent, and the surrounding rock will produce partial radial tensile shear failure. The surrounding rock can still provide the binding force. The influence of surrounding rock is weak. The bond strength provided by the country rock is insufficient, and the effect of the anchoring force on the interface is not obvious; when the strength of the country rock is substantially greater than the strength of the anchorage agent itself, for example, and the country rock is simulated with steel pipe and is approximately non-deformed, the anchorage interface is subjected to axial force through shear failure of the anchorage agent. At this time, the strength of the anchorage agent itself limits the ultimate pull-out strength of the anchor.

According to Mohr–Coulomb theorem,

$$\tau_1 = \sigma \tan \varphi + c. \quad (1)$$

In this forum, τ_1 is the shear strength on the shear plane; $\sigma$is the normal stress on the shear plane; $c$is the rock cohesion; and φ is the internal friction angle of the rock. It can be concluded that different environments lead to different bond strength of surrounding rock; that is, different normal stress on anchorage interface will lead to different failure strength of interface. When the shear stress on the interface exceeds its shear strength, plastic failure occurs at the anchorage interface, and the relative slip between the bolt and the anchoring agent enters the residual strength stage. In this case, only the interface friction force exists on anchorage interface that can be expressed as the following formula:

$$\tau_2 = \sigma \tan\phi. \quad (2)$$

In this forum, σ is the normal stress on the sliding surface and $\phi$is the internal friction angle of rock. It can be seen that the friction force is also directly proportional to the normal stress on the anchorage interface, which is provided by the reaction of surrounding rock. It can be seen from Figure 9 that the residual pull-out force of the anchor body decreased by 46.7% and 56.8%, respectively, at 50°C and 70°C relative to 20°C; the residual tensile strength of C20, C40, and C60 country rock decreased by 51.9%, 38.6%, and 49.4%, respectively, at 50 °C and 60.5%, 61.8%, and 61.6%, respectively, at 70°C relative to 20°C. When the country rock strength is high (steel pipe country rock), it provides a shear force reaction force of the anchor solid interface, the normal stress of the interface is large, and the residual anchoring force of the interface is greater than that of the weak strength of the country rock. With the increase of the temperature, the strength of the anchoring agent itself decreases, and the shear strength of the anchorage interface decreases, so the residual stress of the anchorage solid decreases; in the pull-out specimens of concrete country rock, the country rock cannot provide enough shear force reaction force. Before the shear slip failure of the anchor solid interface, the country rock undergoes radial shear failure, the normal stress of the interface decreases, and the residual anchoring force of the anchor body is small; under the same country rock conditions, the higher the ambient temperature, the smaller the residual stress of the anchor. In general, under the same temperature environment, the higher the strength of country rock, the greater the residual stress of the anchor; under the same strength of country rock, the higher the ambient temperature, the smaller the residual pulling force of the anchor.

4.3. Axial Force Distribution of Bolt under Different Loads. When the anchor body is pulled out axially, the end of the bolt bears the pull-out force along the axial direction of the rod body. The pull-out force is transferred to the whole anchor body along the shear stress form of the interface between the rod and the anchor. The axial deformation of the anchor rod is produced under the action of axial force $P_{(i)}$. According to the strain gauge values at different positions in the bolt body combined with (3), the axial force

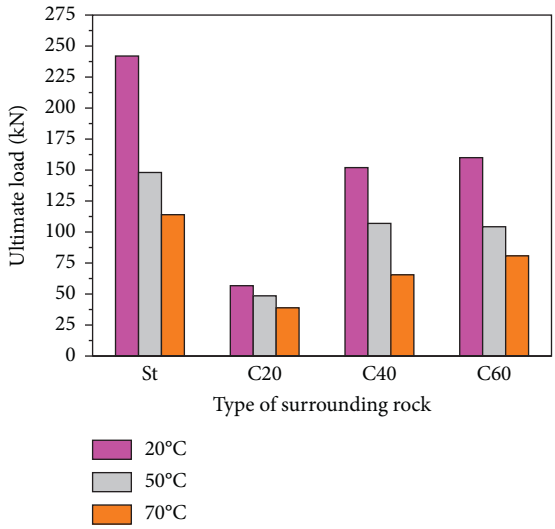

Figure 8: Ultimate pull-out strength of specimens.

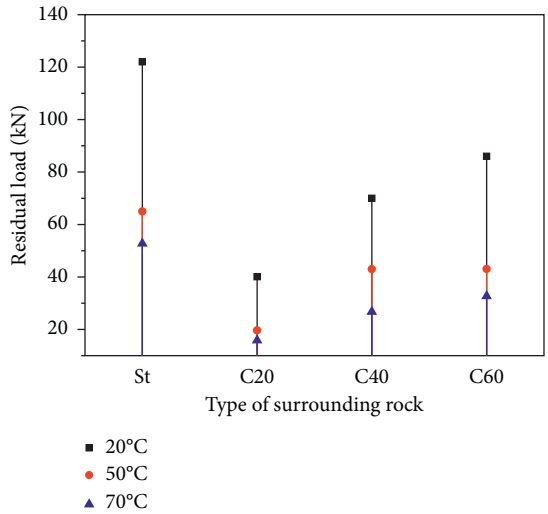

Figure 9: Residual drawing force of specimens.

values at different positions along the bolt axis can be obtained.

$$P_{(i)} = \varepsilon_{(i)} EA. \tag{3}$$

In the above formula, $P_{(i)}$ is the calculated value of the axial force at point i; $\varepsilon_{(i)}$is the measured strain value at point i; E represents the elastic modulus of the test anchor, with a value of 200 GPa; and A is the cross-sectional area of the test bolt, where the area lost due to the installation of the strain gauges is subtracted, to give a value of 344.89 mm^2. For increasing axial load on the anchor rod, the axial force distribution of the anchor under different axial loads is shown in Figure 10.

According to (1), the axial force distribution of the bolt can be obtained by processing the monitoring data. When the simulated ambient temperature is 20, 50, and 70°C, there were 12 test pieces for different country rock strengths. Here, six representative specimens were selected and are drawn as shown in Figure 10.

Figures 10(a)~10(d) show the pull-out monitoring results of specimens with different country rock strength at 50°C. Under the action of different axial loads, the axial force of the bolt decreases with the distance from the pull-out end of the bolt. In the environment of 50°C, when the country rock strength is C20, the pull-out load at the anchorage interface is lower, and the lower pull-out force decreases with the axial extension of the anchor rod. When the pulling force was 40 kN, the tensile force at 2~7# decreased by 15.5%, 34.5%, 67.2%, 90.5%, 97.4%, and 98.6%, respectively. Figures 10(b) and 10(c), respectively, show that the strength of the country rock is C40 and C60. When the pull-out force ratio is small (less than 60 kN), the axial force of anchor rod decreases linearly; with the increase of drawing force, the reduction range of the pulling force increases. When the pull-out force was 100 kN, the tensile force at 2~7# in the C40 specimen decreased by 13.6%, 34.5%, 50.1%, 67.5%, 83.0%, and 92.2%, respectively, while that of the C60 specimen decreased by 14.8%, 31.7%, 42.8%, 66.9%, 81.7%, and 93.5%, respectively. The reduction range of the bolt axial force is the largest in the range of 0~180 mm, but smaller in the range of 180~280 mm. Figure 10(d) shows the anchoring of the steel pipe country rock. When the pull-out force is small (less than 60 kN), the axial force of the anchor rod decreases linearly; when the pull-out force is greater than 160 kN, the stress of the anchor rod at the 2# strain gauge (distance of 20 mm) closest to the pull-out end of bolt is basically equal to the pulling force, indicating that the anchoring agent has reached the shear strength and has been damaged; with the increase of drawing force, the anchoring agent at the 3# strain gauge also reaches the shear strength.

By comparing the test results of different ambient temperatures under the strength of C40 surrounding rock as shown in Figures 10(e), 10(b), and 10(f), it is concluded that when the anchor body is close to the loss of anchor, the axial force at 2~7# in the environment of 20°C decreases by 13.4%, 24.3%, 46.7%, 74.2%, 85.7%, and 93.6%, respectively. At 70°C, the axial forces at 2~7# decreased by 23.5%, 40.1%, 60.2%, 72.5%, 82.2%, and 94.1%, respectively. It can be concluded that with the increase of ambient temperature the axial force distribution of bolt is more uniform.

4.4. Distribution of Axial Shear Force of Bolt under Different Loads. According to the static balance relationship and load transfer principle, the shear force $P_{(i)}$ at the interface between the anchor bolt and anchoring agent at any cross-section of the bolt is equal to the axial force of the bolt. Therefore, the shear stress at the interface of the anchor bolt and anchoring agent can be calculated from the measured values of two adjacent strain gauges; the calculation formula is as follows:

$$\tau_{(i)} = \frac{\left[\varepsilon_{(i)} - \varepsilon_{(i+1)}\right] EA}{\pi d \Delta z}. \tag{4}$$

In the above formula, $\tau_{(i)}$is the average value of shear stress at the anchor bolt-anchorage agent interface between i

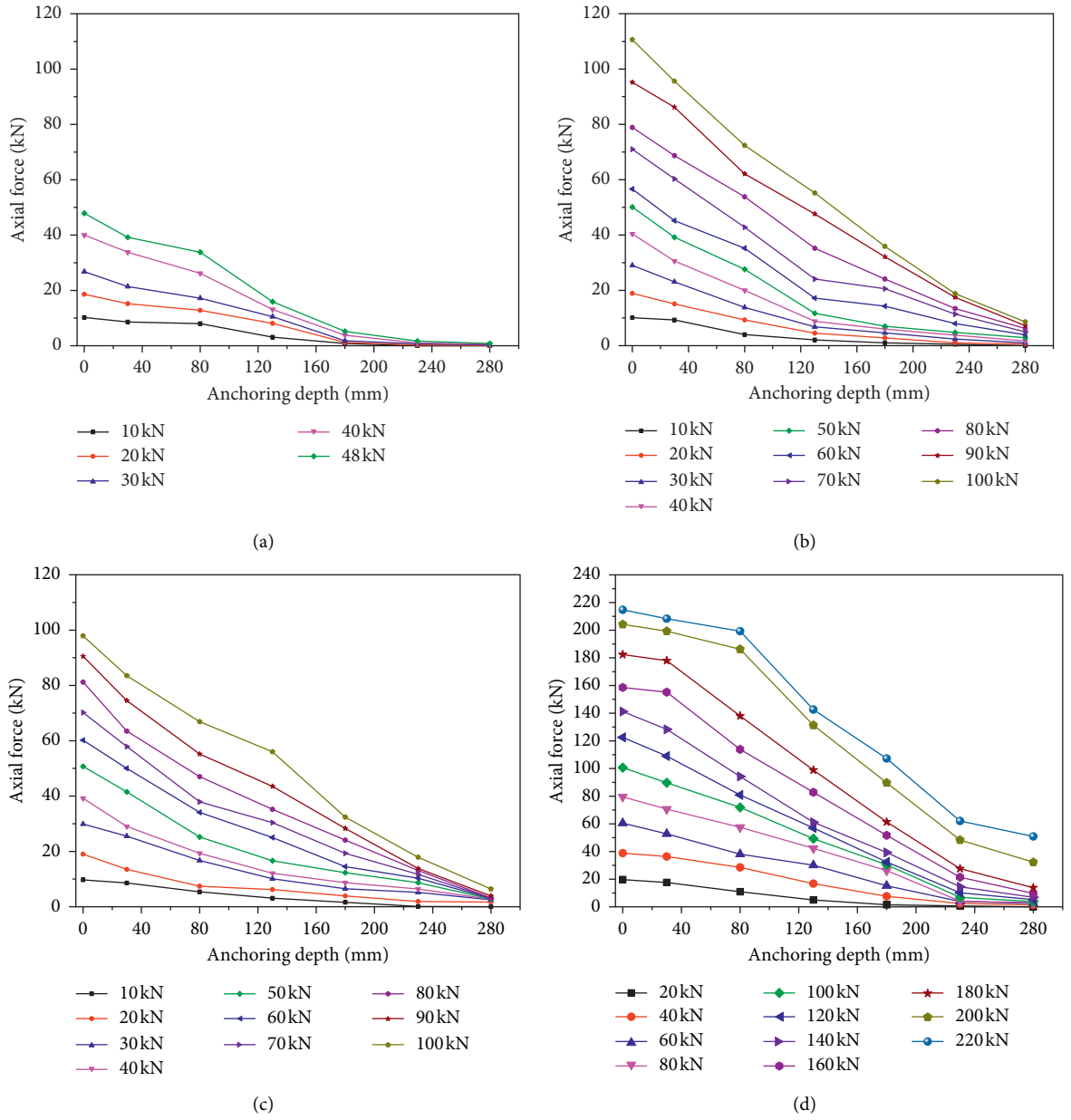

Figure 10: Continued.

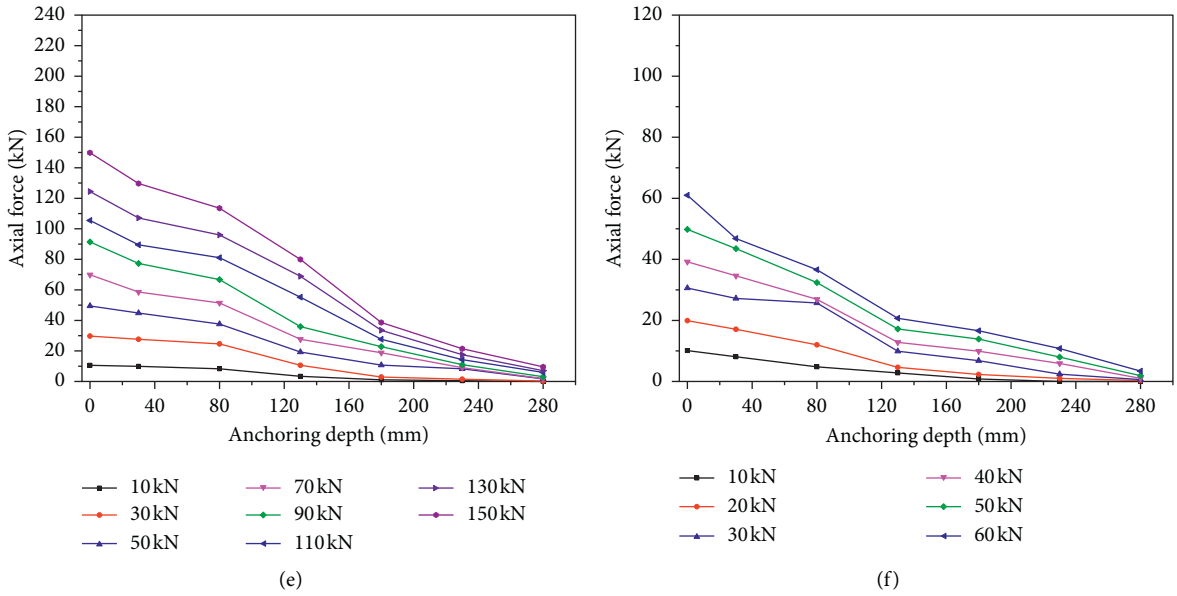

Figure 10: Axial force distribution diagrams under different loads. (a) C20-50°C specimen. (b) C40-50°C specimen. (c) C60-50°C specimen. (d) St-50°C specimen. (e) C40-20°C specimen. (f) C40-70°C specimen.

and $i+1$; $\varepsilon_{(i)}$and $\varepsilon_{(i+1)}$are the strain values measured at points i and $i+1$; $E$is the elastic modulus of the test anchor, with a value of 200 GPa; $A$and d represent the cross-sectional area and diameter of the test bolt, respectively; and Δz is the distance between adjacent strain gauges, with a value of 50 mm. From (4), the change in the shear stress at the anchorage interface along the bolt can be calculated, as shown in Figure 11.

The following can be seen from Figure 11: ① under the action of axial pull-out force, the shear stress of anchorage interface increases rapidly near the anchorage end and then decreases gradually along the direction from the anchorage end to the anchorage bottom until it tends to 0. And with the increase of bolt load, the peak value of interfacial shear gradually shifts from the anchor end to the deep. ② At the same temperature, the maximum shear stress of anchorage interface increases with the increase of surrounding rock strength. The comparison between Figures 11(a) and 11(d) shows that the maximum shear stress is 4.7 MPa when the surrounding rock strength is C20, and 22.6 MPa when the steel pipe is used as the surrounding rock, and the shear stress increases greatly. ③ Under the same surrounding rock strength, the maximum shear stress of anchorage interface decreases with the increase of ambient temperature. Compared with Figures 11(e) and 11(f), it can be seen that the maximum shear stress of the anchorage specimen is 16.42 MPa in the environment of 20°C and 6.3 MPa in the environment of 70°C. The shear stress decreases greatly. ④ The shear stress of the bolt is mainly concentrated in the range of 0~150 mm, and the shear stress in the anchorage section is at a low level when it is greater than 150 mm.

In addition, Figure 11(d) shows the anchoring solid of steel pipe country rock. With the increase of axial force, when the stress exceeds 160 kN, the anchoring interface at the initial end of the anchorage will undergo shear failure. Generally speaking, the different stress-strain properties of the anchorage materials lead to a non-linear distribution of the shear stress at the anchorage interface. Different temperatures and country rock strengths have an impact on the peak value of the shear stress at the anchor interface, but have no effect on the distribution form of the interfacial shear stress. According to the distribution form and transfer law of shear stress at the anchorage interface, it can be concluded that the failure of the anchorage interface is a progressive and irreversible process.

4.5. Analysis of Energy Consumption Value. The value of pull-out energy consumption is the energy consumed when the anchorage specimen is pulled out. This value is the work done to resist the pull-out force of the anchor rod body during the pulling out process. The pull-out energy consumption value of the anchorage body is calculated by the drawing force displacement curve; results are shown in Figure 12.

It can be seen from Figure 12 that when the pull-out specimens are in different ambient temperatures, the value of pull-out energy consumption increases significantly with the increase of country rock strength. According to the analysis, the energy consumption value of the specimens with country rock strength of C20, C40, and C60 decreased by 74.69%, 51.05%, and 38.54%; 63.03%, 45.59%, and 39.99%; and 74.85%, 47.36%, and 45.97%, respectively, compared with the steel tube specimen in the process of anchor rod drawing at 20, 50, and 70°C.

Under the same country rock strength conditions, the pull-out energy consumption decreases with the increase of ambient temperature. Relative to the specimens in the 20°C environment, the energy consumption values of bolt specimens in C20, C40, C60, and steel pipe country rock were

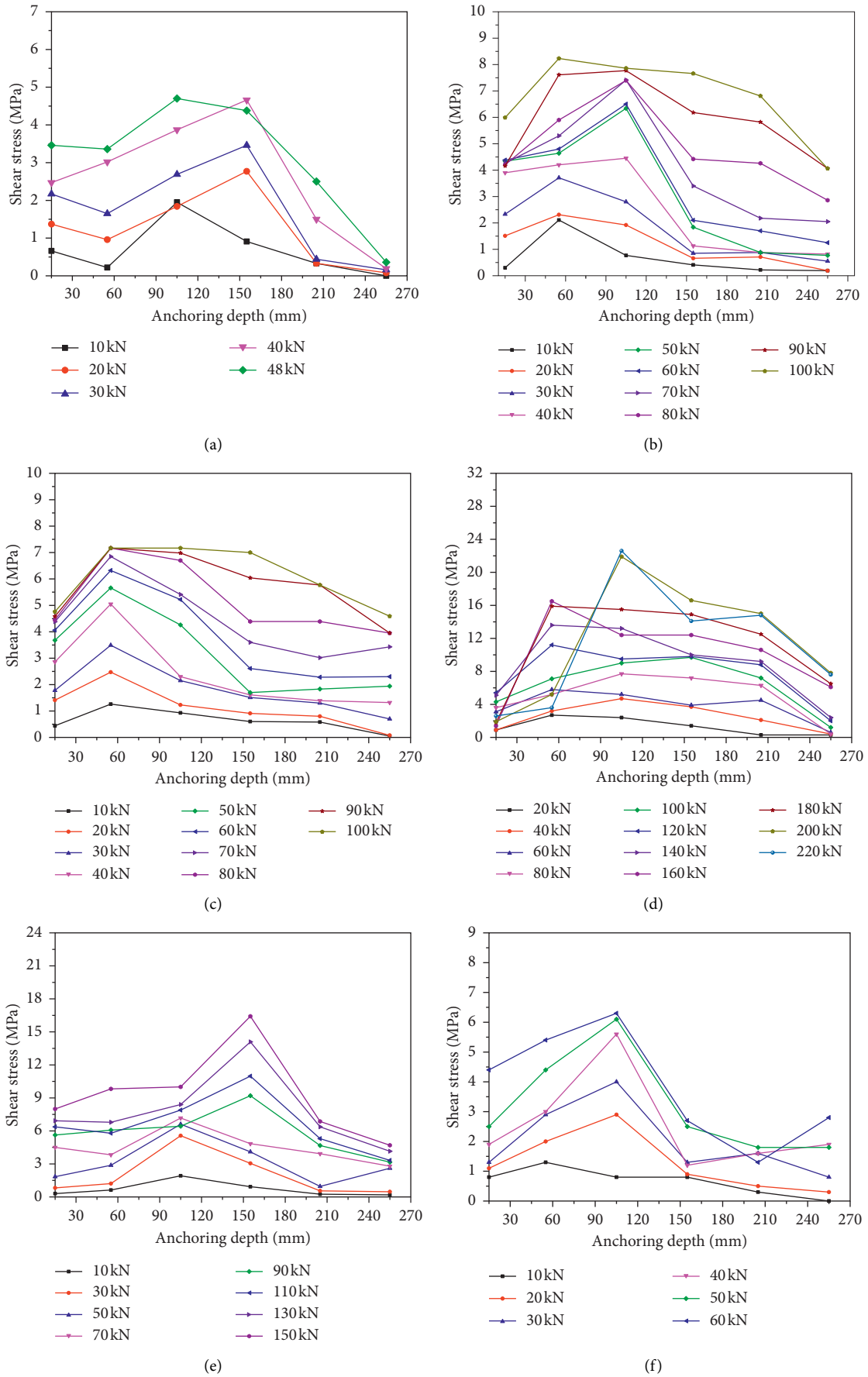

Figure 11: Shear stress distribution diagrams under different loads. (a) C20-50°C specimen. (b) C40-50°C specimen. (c) C60-50°C specimen. (d) St-50°C specimen. (e) C40-20°C specimen. (f) C40-70°C specimen.

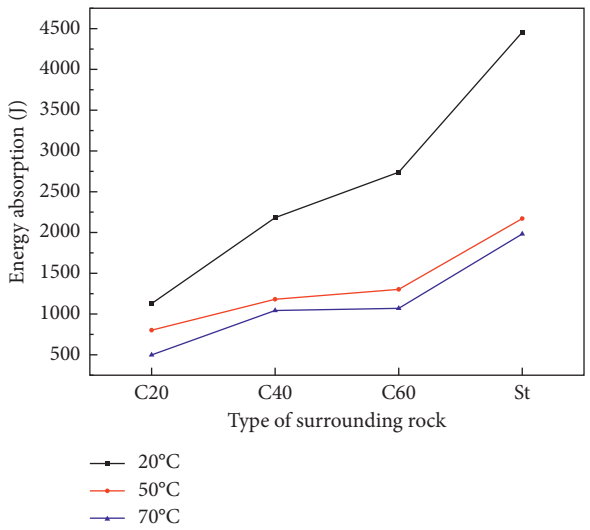

Figure 12: Energy absorption under different temperatures and country rock strength conditions.

reduced by 28.85%, 55.79%, 45.88%, 52.15%, and 52.45%, 60.94%, 51.30%, 55.51%, respectively.

From the above data analysis results, it can be seen that the energy consumption value of the pull-out specimen varies greatly from 20°C to 50°C and less so from 50°C to 70°C. Compared with the medium strength country rock (C40, C60), the soft country rock (C20) or hard country rock (steel pipe) has a greater change in the energy consumption value of the pull-out specimen. When the pull-out specimens are in medium strength country rock, the change of the country rock strength has little influence on the energy consumption value of these specimens. According to the test analysis, the country rock strength and ground temperature have an impact on the bolt support effect. To ensure the bolt support effect, it is necessary to design different anchor support parameters according to the specific support environment.

5. Failure Mechanism Analysis and Experimental Verification of Bolt-Anchoring Agent Interface

It can be seen from Figures 10 and 11 that in the drawing state of the anchor the axial tension at the initial end of the anchor gradually decreases along the interface between the bolt and the anchoring agent. With the increase of axial pull-out force, the shear stress of the anchorage interface gradually spreads to the deep end, resulting in progressive failure of the interface [24–26]. When the pull-out specimen is completely destroyed, the interface between the anchor rod and the anchorage agent on any cross-section will go through elastic stage, failure stage, and sliding friction stage. Therefore, the shear force on the anchorage interface varies with the position and stage [27–30].

The shear resistance of the anchorage interface is composed of adhesive force, mechanical bite force, and friction force. The adhesive force is small and can be ignored generally. The friction force only occurs when shear slip occurs. Therefore, the mechanical bite force is the main factor determining the interfacial shear resistance. Under the action of the bolt surface profile, the mechanical bite force of the interface produces the radial shear force component of the anchorage body. Under the action of axial force and radial shear force, the pull-out specimens have different failure states. Figure 13 and Table 4 show the failure pictures and failure states of the specimens, respectively.

According to the results in Table 4, there is no broken bolt in all the pull-out specimens, which indicates that the strength of the bolt and the rigidity of the drawing die are enough to meet the test requirements. According to the experimental phenomena, the failure modes of the anchor bolt-anchorage agent interface are divided into shear slip mode and shear expansion slip mode, as shown in Figure 14.

When the pull-out specimen is in tension, the anchorage interface produces shear expansion force, which acts on the country rock of the specimen. The strength of surrounding rock itself provides reaction for the shear expansion force of anchorage interface. If the strength of the anchoring agent itself is high, the mechanical bite force of the anchoring interface is large, and the radial shear force is also increased. If the shear failure of the country rock of the specimen before the through shear occurs at the interface, the anchoring interface will produce lateral slip and shear dilatation slip failure, as shown in Figure 14(a); if the strength of the country rock is sufficiently large to provide enough shear expansion reaction force, the through-shear failure occurs at the anchorage interface, which is shear slip failure, as shown in Figure 14(b).

As shown in Figure 14(a), when shear slip failure occurs at the anchorage interface and the axial pull-out force is small, the interface is in an elastic deformation state; with the increase of pull-out load, the anchorage interface produces local extrusion failure, forming a slip surface. According to the stress balance relationship, the normal stress and tangential stress on the slip surface are as follows:

$$\sigma_n^i = \sigma_v \cos i + \frac{P}{A} \sin i, \tag{5}$$

$$\tau^i = \frac{P}{A} \cos i - \sigma_v \sin i. \tag{6}$$

In formulas (5)~(6), Arepresents the conical area at interface failure, $A = \pi (d_b^2 - r^2) \sin i$; $d_b = r + h$, d_b, r, h represent the outer diameter, inner diameter, and rib height of the bolt surface profile, respectively; σ_v is the radial stress of surrounding rock on the anchorage interface; $P$is the axial drawing force; and i is the slip angle of the anchoring interface. With the increase of axial pull-out force, when the shear stress on the sliding surface meets equation (1), the anchoring interface will produce slide. Substituting (5) and (6) into (1), eliminating σ_n^i and τ^i, the following formula is obtained:

$$P = \pi\left(d_s^2 - r^2\right)\left[\frac{\cos \phi}{\sin i \cos (i + \phi)} c + \frac{\sigma_v \tan (i + \phi)}{\sin i}\right]. \tag{7}$$

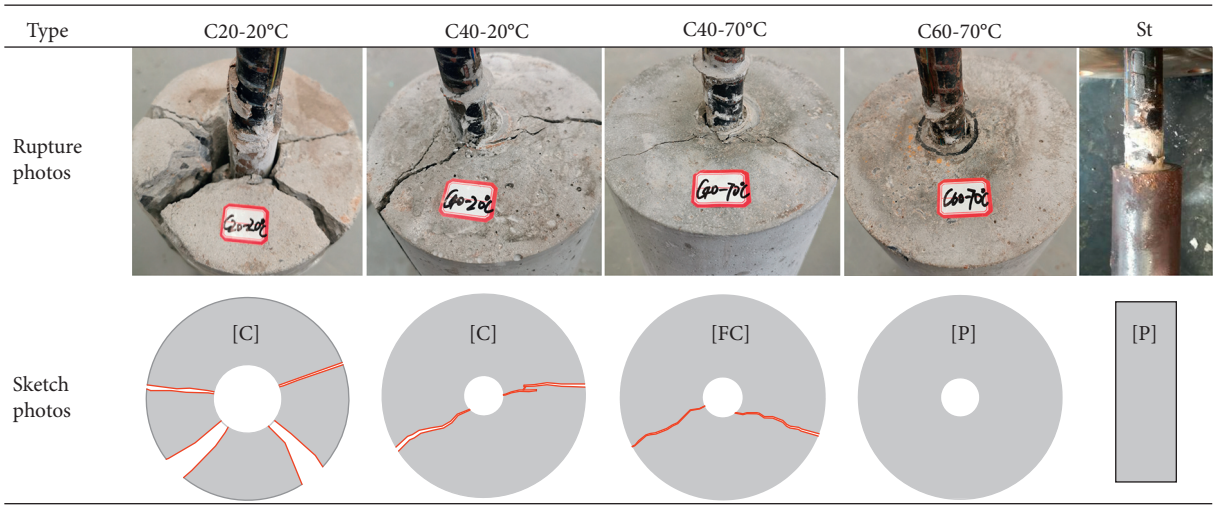

Figure 13: Failure mode of anchor loss of pull-out specimens.

Table 4: Damage forms of samples.

(°C)	C20	C40	C60	St
20	C	C	C	P
50	C	C	C	P
70	C	FC	P	P

C is the country rock cracking; P is the bolt pulling out; FC indicates a small number of cracks at the orifice.

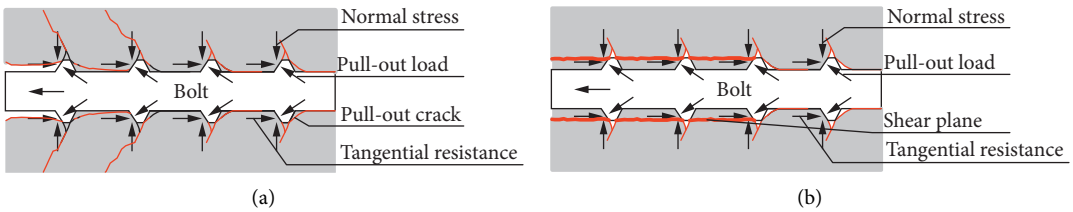

Figure 14: Failure modes of anchorage interface: (a) shear expansion slip mode; (b) shear slip mode.

It can be seen from formula (7) that the sliding resistance of anchorage interface is composed of two parts: one is the cohesion of anchorage agent itself and the other is the radial restraint of surrounding rock. The interface dilatancy will lead to the expansion of the inner wall of the surrounding rock anchor hole, resulting in cracks in the inner wall of the anchor hole. When the shear stress of the inner wall of the cylinder reaches its tensile strength, the radial tensile shear failure of the inner wall will occur. Therefore, according to Lame's solution [31], when the inner wall of surrounding rock enters the critical point of tensile shear failure, the tensile stress of surrounding rock on the anchorage interface is in equilibrium with the radial dilatancy force produced by drawing. It will get the following formula:

$$p_0 = \frac{\left(d_0^2 - d_b^2\right)\sigma_L + 2d_0^2\sigma_w}{d_0^2 + d_b^2}. \tag{8}$$

In formula (8), p_0 is the radial stress on the anchoring interface; d_0 is the outer diameter of the anchoring body; σ_w is the external confining pressure on the anchoring body; and σ_L is the crack compressive strength of internal wall of anchorage interface, which is 2.5~3 times of the tensile strength obtained by the uniaxial direct drawing method [32].

When the anchorage interface is in the critical state of shear expansion crack initiation, the radial stress of the surrounding rock at the interface is equal to that of the surrounding rock on the slip surface; that is,

$$p_0 = \sigma_v. \tag{9}$$

By substituting (8) and (9) into equation (7), and considering the attenuation of mechanical properties of anchoring agent layer under the action of temperature, the following results are obtained:

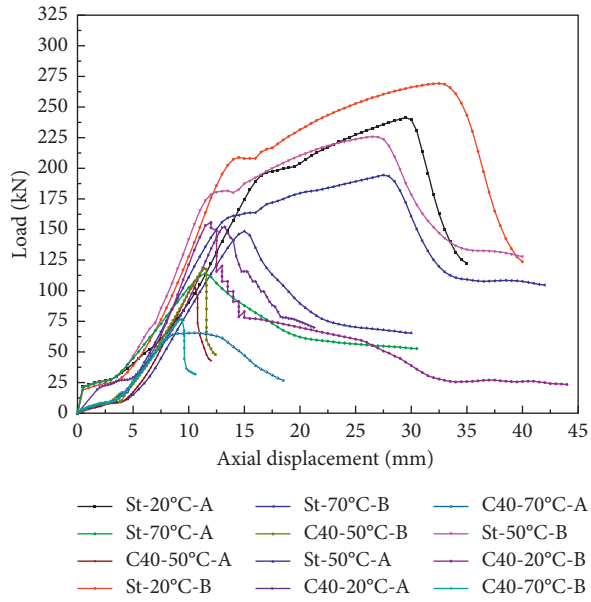

Figure 15: Relationship between drawing force and displacement.

$$P_{\max} = \pi\left(d_s^2 - r^2\right)\left[\frac{\cos\phi_T}{\sin i\cos\left(i+\phi_T\right)}c_T + \frac{\left[\left(d_0^2 - d_b^2\right)\sigma_L + 2d_0^2\sigma_w\right]\tan\left(i+\phi_T\right)}{\sin i\left(d_0^2 + d_b^2\right)}\right]. \tag{10}$$

In the drawing test of C40-50°C specimen, the surrounding rock is not affected by external confining pressure. The parameters are as follows: external confining pressure σ_w is zero, the shear slip angle $i = 7^\circ$, anchor parameters d_s and r are 22 mm and 19.2 mm, respectively, surrounding rock diameter d_0 is 150 mm, σ_L is 6.8 MPa, and the measured internal friction angle and cohesion of anchoring agent are 38° and 8.5 MPa, respectively. The above parameters are substituted into formula (10).The results show that the maximum axial load is 47.52 kN, which is 45.7% of the ultimate axial load and this is less than 50% of the ultimate pull-out load in [33]. From formula (10), it can be concluded that the low strength of surrounding rock can provide less σ_L, the anchorage interface will produce radial expansion crack, the interface shear slip angle will be larger, and the ultimate axial load will be reduced. Therefore, the strength of anchorage agent should match the strength of surrounding rock. The greater the strength of surrounding rock is, the better the performance of anchorage agent can be used.

However, with the increase of the ambient temperature, temperature stress is produced inside the drawing specimen and the mechanical properties of the component materials are changed [34, 35]. Due to the small heating range of the simulated ground temperature environment test, the difference of thermal expansion coefficient between concrete and anchor rod is small, so the temperature stress in the specimen could be ignored [36, 37]. The relevant literature shows that the mechanical properties of the concrete and bolt are almost unchanged within the range of 100°C, but the mechanical properties of the anchoring agent decrease greatly. It can be seen that the resin anchoring agent is the most sensitive to the temperature change in the anchoring solid. To summarize, it can be concluded that the bolt supporting effect can be effectively improved by pulling the specimen in a high-temperature environment and improving the strength of the resin anchoring agent. Furthermore, the matched country rock strength should also be considered. By adjusting the strength of the anchoring agent and the country rock, the failure mode of the anchorage interface changes from shear dilatancy slip mode to shear slip mode, thus achieving maximum utilization of the anchoring force.

In order to verify the rationality of the above-mentioned interface failure mechanism and clarify the reasonable way to improve the anchorage interface load, we select the self-made high-strength, heat-resistant anchorage agent for indoor pull-out test, and compare the experimental results with the test results of conventional anchorage agent, as shown in Figure 15 (A represents the conventional anchorage agent; B represents the new anchorage agent). The mechanical parameters of self-made new anchoring agent at different temperatures are shown in Table 5 and C40 concrete and steel pipe are selected for surrounding rock [38]. The fabrication, curing, and testing procedures of the specimens are as described in Section 2.

It can be seen from Figure 15 that with the increase of the ambient temperature relative to 20°C the ultimate pull-out force of the new anchorage agent specimen at 50°C and 70°C decreases by 28.85% and 55.79%, respectively, with the increase of ambient temperature. Therefore, with the increase of ambient temperature, the reduction extent of the ultimate pull-out force of the new anchorage agent specimen

Table 5: Compressive strength of the anchoring agent in different temperature environments.

Type	20°C (MPa)	50°C (MPa)	80°C (MPa)	110°C (MPa)
New	73	69	60	50.6

is significantly smaller than that of the conventional anchorage agent specimen under the same temperature environment. However, in the case of C40 country rock, with the increase of ambient temperature the change range of the ultimate pull-out force of the new anchorage agent specimen is smaller than that of the conventional anchorage agent specimen. It can be seen that if the strength of the country rock is not high in a high-temperature environment, the supporting performance of the bolt cannot be improved by only improving the strength of the anchoring agent.

Therefore, in order to ensure the effectiveness of bolt support in high temperatures and weak or broken rock, it is necessary not only to improve the stability of the mechanical properties of the anchoring agent in high-temperature environments, but also to improve the strength of the country rock by grouting and other means, so that the high-strength anchoring agent will eventually produce interfacial shear slip failure. In addition, some deficiencies remain in the above analysis: the anchor body in deep stratum is in an environment of high geostress, high ground temperature, and weak rock stratum, the failure limit of the country rock changes under the action of high stress, and the indoor pull-out test does not consider the influence of crustal stress environment on the failure of anchorage interface. Further research of these issues will be carried out in the future.

6. Conclusion

In this paper, C20, C40, C60 strength concrete and steel pipe are used to simulate different surrounding rock strength environment, and indoor anchor pull-out tests are carried out at 20°C, 50°C, and 70°C. The following can be concluded:

(1) Based on the analysis of pull-out test results under different environments, the failure process of the bolt interface is divided into four stages: elastic stage, plastic yield stage, anchor loss failure stage, and residual stress stage. For the test anchorage length, with the weakening of country rock strength or the increase of ambient temperature, the country rock is prone to split failure or the shear strength of the anchoring agent is reduced. At this time, the plastic yield stage of the anchorage interface is either not obvious or non-existent.

(2) Through the pull-out test, it is concluded that the ultimate pull-out force and residual anchoring force of the anchorage interface increase with the increase of surrounding rock strength when the ambient temperature is the same; when the surrounding rock strength is the same, the increase of temperature leads to the weakening of the anchoring force of the anchorage interface. Combined with the shear stress inversion of the anchorage interface, it is concluded that the strength and temperature of surrounding rock only change the magnitude of the interface anchorage force but do not change the interface stress transfer law. With the increase of drawing load, the peak shear stress of interface transfers to the anchorage end.

(3) The results show that the value of energy consumption increases significantly with the increase of country rock strength, and the energy consumption value varies greatly from 20°C to 50°C and less from 50°C to 70°C. Compared with the medium strength country rock (C40 and C60), the energy consumption value of the pull-out specimen changes significantly in soft country rock (C20) or hard country rock (steel pipe). When the pull-out specimen is in medium strength country rock, the change of country rock strength has little effect on the energy consumption value of the specimen.

(4) According to the pull-out test data and the failure phenomenon of the specimen, it is concluded that the failure modes of the anchor bolt-anchorage agent interface can be divided into two types: shear slip mode and shear expansion slip mode. By comparing the test results of a high-strength and temperature-resistant anchorage agent, it is concluded that improvement of the anchoring performance of the anchor bolt-anchorage agent interface needs to consider the adjustment of the strength of the anchoring agent and the country rock. Thus, the failure mode of the anchor interface is changed from shear expansion sliding mode to shear slip mode and maximum use of anchoring force is achieved.

Data Availability

The data used to support the findings of this study are included within the article.

Conflicts of Interest

The authors declare no conflicts of interest.

Authors' Contributions

Xiaohu Liu and Zhishu Yao contributed to conceptualization; Weipei Xue and Xianwen Huang performed formal analysis; Xiaohu Liu contributed to methodology and writing (original draft); Xuesong Wang provided resources.

Acknowledgments

This research was supported by the Anhui University discipline professional talented person (No. gxbjZD09), Anhui Provincial Natural Science Foundation Youth Project (1908085QE185), Anhui Provincial College of Natural Science Research Key Project (KJ2018A0098), project funded by China Postdoctoral Science Foundation (2018M642502), and the Science Research Foundation for Young Teachers in Anhui University of Science and Technology (QN2017211).

References

[1] M. He, H. Xie, and S. Peng, "A study of deep mining rock mechanics and engineering disaster control," *Mine Support*, vol. 3, pp. 1–14, 2007.

[2] Z. Zhang, Y. Liu, J. Teng, H. Zhang, and X. Chen, "An investigation into bolt anchoring performance during tunnel construction in bedded rock mass," *Applied Sciences*, vol. 10, no. 7, p. 2329, 2020.

[3] B. Indraratna and P. K. Kaiser, "Analytical model for the design of grouted rock bolts," *International Journal for Numerical and Analytical Methods in Geomechanics*, vol. 14, no. 4, pp. 227–251, 1990.

[4] Y. Cheng, Q. Meng, G. Xu, and H. Wu, "Bolt-grouting combined support technology in deep soft rock roadway," *International Journal of Mining Science and Technology*, vol. 6, pp. 1–9, 2016.

[5] X. Feng, N. Zhang, G. Li, and G. Guo, "Pullout test on fully grouted bolt sheathed by different length of segmented steel tubes," *Shock and Vibration*, vol. 2017, p. 16, Article ID 4304190, 2017.

[6] Q. Wang, Q. Qin, B. Jiang, H. C. Yu, R. Pan, and S. C. Li, "Study and engineering application on the bolt-grouting reinforcement effect in underground engineering with fractured surrounding rock," *Tunnelling and Underground Space Technology*, vol. 84, pp. 237–247, 2019.

[7] H. Kang, "Sixty years development and prospects of rock bolting technology for underground coal mine roadways in China," *Journal of China University of Mining & Technology*, vol. 45, pp. 1071–1081, 2016.

[8] H. Kim, H. Rehman, W. Ali et al., "Classification of factors affecting the performance of fully grouted rock bolts with empirical classification systems," *Applied Sciences*, vol. 9, no. 22, p. 4781, 2019.

[9] A. Çolak, "Parametric study of factors affecting the pull-out strength of steel rods bonded into precast concrete panels," *International Journal of Adhesion and Adhesives*, vol. 21, no. 6, pp. 487–493, 2001.

[10] J. Long, "The mechanism of synergetic anchorage in deep roadway surrounding rock," *Journal of Mining & Safety Engineering*, vol. 33, pp. 19–26, 2016.

[11] S. Zhang, P. Gou, and H. Fan, "Influence of water and temperature on resin anchor-hold," *Journal of Southeast university (Natural Science Edition)*, vol. 35, pp. 49–54, 2005.

[12] B. Hu, H. Kang, J. Lin, and J. Cai, "Study on influence of temperature on anchorage performance of resin anchored bolt," *Journal of Mining & Safety Engineering*, vol. 29, pp. 644–649, 2012.

[13] X. Zhao, H. Zhang, M. Zhang, and H. Zhang, "Optimisation of bolt rib spacing and anchoring force under different conditions of surrounding rock," *Rock and Soil Mechanics*, vol. 39, pp. 1263–1280, 2018.

[14] F. Li, X. Quan, Y. Jia, B. Wang, G. Zhang, and S. Chen, "The experimental study of the temperature effect on the interfacial properties of fully grouted rock bolt," *Applied Sciences*, vol. 7, no. 4, p. 327, 2017.

[15] F. Li, H. Jin, D. Hu, B. Wang, and Y. Jia, "Influence of temperature and roughness of surrounding rocks on mechanical behavior of rock bolts," *Soil Dynamics and Earthquake Engineering*, vol. 103, pp. 55–63, 2017.

[16] S. Xue-gui, D. Xian-jie, Y. Hong-hu, and L. Ben-kui, "Research of the thermal stability of structure of resin anchoring material based on 3D CT," *International Journal of Adhesion and Adhesives*, vol. 68, pp. 161–168, 2016.

[17] L. Ming-jing, "Research on thermo-mechanical coupling properties of resin anchorage system in deep mine roadway," *Doctoral thesis*, Anhui University of Science & Technology, Anhui, China, 2013.

[18] T. Pothisiri and P. Panedpojaman, "Modeling of bonding between steel rebar and concrete at elevated temperatures," *Construction and Building Materials*, vol. 27, no. 1, pp. 130–140, 2012.

[19] S. Chen, "Study on the mechanical properties of wholly grouted anchor in thermal damage tunnel," Master Degree Thesis, Southwest Jiaotong University, Chengdu, China, 2016.

[20] Z. Y. Hu and S. M. Wang, "Systematic study on influencing factors of main performance indexes of resin anchoring agent," *Science and Technology Economic Guide*, vol. 19, pp. 78-79, 2017.

[21] X. Liu, Z. Yao, W. Xue, and Li Xiang, "Effect of temperature and accelerator on gel time and compressive strength of resin anchoring agent," *Advances in Polymer Technology*, vol. 2019, Article ID 3546153, 11 pages, 2019.

[22] L. Yang, Z. Yao, W. Xue, X. Wang, W. Kong, and T. Wu, "Preparation, performance test and microanalysis of hybrid fibers and microexpansive high-performance shaft lining concrete," *Construction and Building Materials*, vol. 223, pp. 431–440, 2019.

[23] Z. Yao, W. Xue, and H. Chen, "Research and application of composite shaft with inner steel plate and high strength reinforced concrete infrozen wellbore," *Journal of Mining and Safety Engineering*, vol. 35, pp. 663–669, 2018.

[24] J. Zou and P. Zhang, "Analytical model of fully grouted bolts in pull-out tests and in situ rock masses," *International Journal of Rock Mechanics and Mining Sciences*, vol. 113, pp. 278–294, 2019.

[25] M. Huang, J. Li, M. Zhao, and C. Chen, "Full-range analysis on mechanical characteristics of bolts in rock mass with bedding separation," *Chinese Journal of Rock Mechanics and Engineering*, vol. 9, pp. 2177–2184, 2017.

[26] I. W. Farmer, "Stress distribution along a resin grouted rock anchor," *International Journal of Rock Mechanics and Mining Sciences & Geomechanics Abstracts*, vol. 12, no. 11, pp. 347–351, 1975.

[27] F. F. Ren, Z. J. Yang, J. F. Chen, and W. W. Chen, "An analytical analysis of the full-range behaviour of grouted rockbolts based on a tri-linear bond-slip model," *Construction and Building Materials*, vol. 24, no. 3, pp. 361–370, 2010.

[28] P. K. Kaiser, S. Yazici, and J. Nose, "Effect of stress change on the bond strength of fully grouted cables," *International Journal of Rock Mechanics & Geomechanical Abstracts*, vol. 29, no. 3, pp. 293–306, 1992.

[29] J. Chen, S. Saydam, and P. C. Hagan, "An analytical model of the load transfer behavior of fully grouted cable bolts," *Construction and Building Materials*, vol. 101, pp. 1006–1015, 2015.

[30] A. J. Hyett, W. F. Bawden, and R. D. Reichert, "The effect of rock mass confinement on the bond streght of fully grouted cable bolts," *IInternational Journal of Rock Mechanics and Mining Science & Geomechanics Abstracts.*vol. 29, no. 5, pp. 503–524, 1992.

[31] Z. Xu, *Elastic Mechanics*, Higher Education Press, Beijing, China, 2006.

[32] J. Wu and M. Wu, "Experimental pesearch of rock fracture under pore-triaxial stress condition," *Seismology and Geology*, vol. 8, no. 2, pp. 69–76, 1986.

[33] C. Cao, T. Ren, C. Cook, and Y. Cao, "Analytical approach in optimising selection of rebar bolts in preventing rock bolting

failure," *International Journal of Rock Mechanics and Mining Sciences*, vol. 72, pp. 16–25, 2014.

[34] W. Yao and J. Pang, "The status and progress of the research on thermal environment of deep mine in China," *Mining Safety & Environmental Protection*, vol. 45, pp. 107–111, 2018.

[35] L. Yuan, "Theoretical analysis and practical application of coal mine cooling in Huainan mining area," *Journal of Mining & Safety Engineering*, vol. 24, no. 3, pp. 298–301, 2007.

[36] J. Li, "Analysis of bond performance between steel reinforcing bars and CFRP layer to concrete under high temperature," *Doctoral thesis*, Harbin Institute of Technology, Harbin, China, 2014.

[37] C. Wang, Y. ou, and J. Huo, "Experimental study on bond performance between steel bar and concrete under high temperature," *Bulletin of the Chinese Ceramic Society*, vol. 36, no. 12, pp. 3984–3992, 2017.

[38] L. Xiao-hu, Z.-shu Yao, X. Wei-pei, and Li Xiang, "Development, performance, and microscopic analysis of new anchorage agent with heat resistance, high strength, and full length," *Journal of Mining & Safety Engineering*, vol. 2019, Article ID 4239486, 9 pages, 2019.